

# Ocean surface temperature- and colour studies from satellites

JAN-PETTER PEDERSEN



Pedersen, J.-P. 1990: Ocean surface temperature- and colour studies from satellites. *Polar Research* 8, 3-9.

This paper introduces satellite remote sensing of sea-surface temperatures and ocean colour studies. The basic radiative transfer equations and available satellite sensor systems are presented. The final part of the paper focuses on temperature applications. Sea surface temperature data derived from available satellite data are presented and discussed.

*Jan-Petter Pedersen, Department of Information Technology, Foundation of Applied Research at the University of Tromsø (FORUT), P.O. Box 2806 Elverhøy, N-9001 Tromsø, Norway; February 1989 (revised June 1989).*

The role of satellites in the monitoring of conditions of the Earth's atmosphere and surface is becoming increasingly important. Satellite measurements are particularly useful in disciplines such as oceanography and meteorology/climatology. Due to the frequent and the simultaneous large area coverage, vast areas of ocean and atmosphere can be studied simultaneously.

Oceanographic applications of satellite remote sensing mainly include studies of surface parameters such as: temperatures, currents, winds and waves. Also of interest are studies of ocean colour which is an index of (near) sub-surface parameters such as ocean productivity and/or concentrations of suspended material.

The application areas of a remote sensor are mainly determined from the operational characteristics of the sensor. The remote sensing of ocean colour requires that the sensor can detect the radiation coming from below the ocean surface. This radiation carries information about sub-surface chemical and/or physical conditions. Such radiation is present in narrow spectral bands in the blue and the blue-green part of the electromagnetic spectrum (Swain & Davis 1978). It is therefore a requirement that an ocean colour observing sensor must operate narrow spectral bands in the blue/blue-green part of the spectrum.

The surface temperature determines the thermal infrared radiation emitted from the sea. The radiation is emitted according to Planck's radiation law (Swain & Davis 1978). The surface temperature is observable by a remote sensor operating in the thermal infrared, or in the microwave part of the electromagnetic spectrum.

Application of traditional oceanographic methods in combination with satellite remote sensing has proved a high degree of correlation between the observed sea surface temperature and the near sub-surface productivity. The areas of highest productivity normally correspond to the areas of lowest surface temperatures (NASA 1984b). Regions of strong tidal mixing and upwelling of deeper water appear as local cool areas exposing different temperature gradient patterns. The temperature gradients (fronts) reflect the physical processes (currents and mixing) which affect the local biological productivity. Ocean colour information derived from spaceborne data has been used by fishermen off the coast of California as a tool for increasing the tuna catches (NASA 1984c). In addition to fish stocks, areas of enhanced productivity have been observed as feeding areas for marine birds and other predators (Schneider this volume).

## Radiative transfer equations

The radiance detected by a remote sensor is comprised of different components, originating from different parts of the total sensor-atmosphere-ocean system:

- the radiance originating from the atmosphere (atmospheric)
- the radiance reflected at the ocean surface (reflected)
- the radiance originating from and below the surface (emitted)

The individual component contribution to the

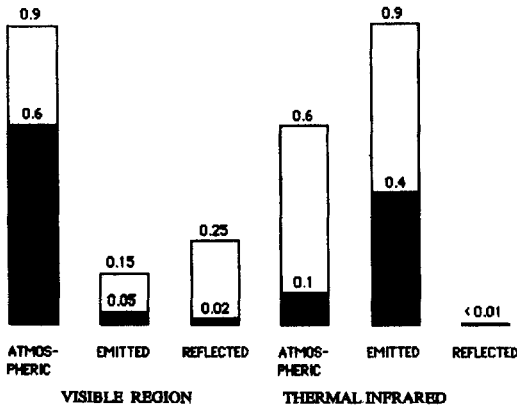


Fig. 1. Components of the total signal detected by a remote sensor in the visible and in the thermal infrared wavelength regions. The numbers indicate the relative fractional contribution limits for the different components (Maul 1981).

total signal is strongly wavelength dependent. Fig. 1 illustrates schematically the fractional component contribution to the total signal at the visible and the thermal infrared wavelength regions. The numbers indicate the relative fractional contribution limits for the different components. The figure shows that in the visible region the atmospheric component of the total detected signal will comprise 60–90%. When dealing with quantitative remote sensing of ocean near-surface conditions, the interesting component is that representing the near-surface emission. This means that the components representing the atmospheric contribution and the surface reflection have to be quantified and compensated for.

#### The equation of radiative transfer

The electromagnetic radiative transfer in a sensor-atmosphere-ocean system can be described mathematically by the equation of radiative transfer. This equation describes all effects inherent upon the electromagnetic radiation. Of special importance are the effects of the atmosphere (attenuation) between the sensor and the measured surface. The atmospheric attenuation depends on the wavelength of the electromagnetic radiation and the composition of the atmosphere along the sensor's line of sight.

The complete form of the equation of radiative transfer is complicated (Liou 1980), and only a

simplified component version of the equation is presented here (Pedersen 1987):

$$R(\lambda, h, \mu, \phi) = \tau(\lambda, h, \mu, \phi)[R_R(\lambda, h, \mu, \phi) + R_E(\lambda, h, \mu, \phi)] + R_P(\lambda, h, \mu, \phi) \quad (1)$$

where

$R(\lambda, h, \mu, \phi)$  = the radiance detected by a sensor at altitude  $h$ , at a given wavelength  $\lambda$ , in the direction ( $\mu = \cos^{-1}\theta, \phi$ ).  $\theta, \phi$  represent the zenith and azimuth angles, respectively.

$R_R(\lambda, h, \mu, \phi)$  = the radiance component due to reflection of solar radiation at the surface.

$R_E(\lambda, h, \mu, \phi)$  = the radiance emitted from the surface.

$R_P(\lambda, h, \mu, \phi)$  = the atmospheric radiance (emitted and reflected).

$\tau(\lambda, h, \mu, \phi)$  = the atmospheric attenuation of the surface radiance.

Solving equation (1) implies applications of proper boundary conditions at the top of the atmosphere, at the atmosphere-ocean interface and at the sea bottom (if visible) (Guzzi et al. 1987). In practice this means that the equation is almost impossible to solve without any simplifications.

The simplifications of the complete equation are strongly dependent upon the actual wavelength bands applied. For example, Fig. 1 shows that a quantitative application of the emitted radiance component in the visible region requires that the dominating atmospheric component must be determined and corrected for (Pedersen 1987). In this region the surface reflection will also contribute significantly.

A similar application in the thermal infrared region means that the reflected component can be ignored without introducing any significant errors (cf. Fig. 1). The atmospheric component is also less dominating in this region. Compared to the visible region, the atmospheric contribution is more easily determined in the thermal infrared region (Pedersen 1982, 1987). The quantitative expressions are outside the scope of this paper.

#### Available satellite sensors

The NOAA-series of polar orbiting, sunsynchronous satellites from which data are read out at

Tromsø Satellite Station (TSS), offer the opportunity to study surface phenomena in arctic regions with a high frequency of repetition. The primary sensor of the NOAA satellites is the Advanced Very High Resolution Radiometer (AVHRR) observing in the visible and in the thermal infrared region. The thermal infrared data from the NOAA satellites are frequently used for studying currents and the sea surface temperatures (SST). The spatial resolution of the NOAA-data of 1 km limits their application to open ocean areas. The new generation of satellites represented by the Landsat/Thematic Mapper (TM) offers, however, the opportunity to study surface phenomena at an increased spatial resolution. Compared to the NOAA satellites, the 120 meter resolution of the TM thermal channel is more adaptable for coastal-zone applications. The important operating characteristics for the satellites are presented in Table 1. The Landsat satellites also operate another visible/near-infrared radiometer, the Multispectral Scanner (MSS). Due to the spectral location and bandwidth of the MSS bands, this radiometer is not suitable for quantitative ocean colour applications.

Until now, there has been only one operational satellite dedicated to ocean colour studies. This satellite, NIMBUS-7, was launched in 1978, and was operational for about five years. The ocean colour sensor on board NIMBUS-7 was a passive radiometer, CZCS (Coastal Zone Colour Scanner), operating at narrow visible and near-infrared spectral bands (see Table 1). The spatial resolution of the sensor was 800 meters, which again limits the applications mainly to open oceans. Sensors analogue to the CZCS are plan-

ned to be put on future Earth observation platforms. These sensors will, however, not become operational until the mid-1990s.

## Geophysical satellite data applications

### *Ocean colour studies*

During its operational lifetime, data from NIMBUS/CZCS were applied for a number of ocean colour studies (Gordon & Clark 1980; Sturm 1982; Gordon et al. 1983). CZCS data have, however, not been applied for quantitative ocean colour studies in Norway.

A study presented by Gordon et al. (1983) discussed the application of CZCS data for the determination of phytoplankton pigment concentrations in the Middle Atlantic Bight off the East Coast of the USA and in the Sargasso Sea. The pigment concentrations determined from satellite images were compared to measurements performed by ships. The results obtained suggested that over the 0.08–1.5 mg/m<sup>3</sup> range, the error in the retrieved pigment (mainly Chlorophyll a) concentration is of the order 30–40% for a variety of atmospheric conditions. Fig. 2 shows a comparison of ship and CZCS measured pigment concentrations (Gordon et al. 1983).

The main problem in ocean colour studies is to obtain a correct atmospheric correction. The atmosphere is a strongly varying medium both in time and space, and these variations are hardly described by any given law. The variations must therefore rely on observations. There exists no

Table 1. Actual ocean colour/temperature observing satellites operational characteristics.

	AVHRR	TM	CZCS
Spectral bands ( $\mu\text{m}$ )	0.58–0.68 0.70–1.1 3.55–3.93 10.3–11.3 11.5–12.5	0.45–0.52 0.53–0.60 0.63–0.69 0.76–0.90 1.55–1.75 2.08–2.35 10.4–12.5	0.43–0.45 0.51–0.53 0.54–0.56 0.66–0.68 0.70–0.80 10.50–12.50
Spatial resolution	1 × 1 km	30 × 30 m 120 × 120 m thermal IR	0.8 × 0.8 km
Swath width	c. 2,500 km	185 km	c. 2,500 km
Operational status	Active	Active	Passive

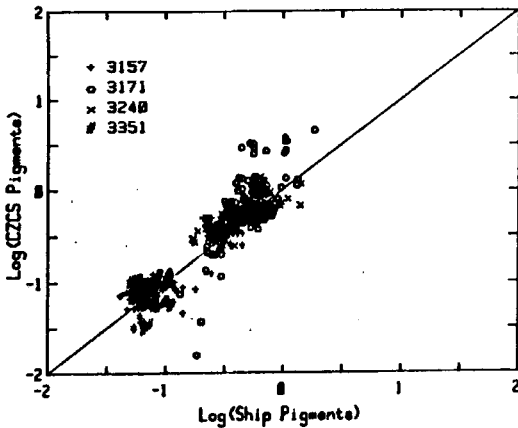


Fig. 2. Comparisons of ship and CZCS measured pigment concentrations for four different NIMBUS orbits (3157, 3171, 3240, 3351) (Gordon et al. 1983).

developed observation network in ocean areas, and present satellite sensors do not give the radiometric accuracy necessary for operational atmospheric corrections of high quality.

#### *Sea-surface temperature studies*

The thermal channels of the AVHRR and the TM are to be considered for this application. The AVHRR 10.3–11.3  $\mu\text{m}$ , the 11.5–12.5  $\mu\text{m}$  channels, and the TM 10.4–12.5  $\mu\text{m}$  channel are all in the same part of the electromagnetic spectrum. Notice, however, that the spectral width of the TM channel is twice that of the AVHRR channels. Due to the spectral coincidence of the TM and AVHRR channels, they are applicable for comparable studies of sea surface temperatures. According to the pre-launch specifications, the temperature sensitivities are  $<0.12\text{ K}$  and  $0.5\text{ K}$  at a surface temperature of  $300\text{ K}$  for the AVHRR and TM, respectively (NASA 1984a; Schwalb 1979).

The most significant difference between the channels is their spatial resolution, 120 meters for TM compared to 1 km for AVHRR. The spatial resolution of the AVHRR limits its applications primarily to open oceans. For studies in the coastal zone and within the fjords, the TM thermal channel is the most suitable.

Different algorithms have been proposed for retrieval of sea surface temperatures (SST) from thermal infrared satellite data. These algorithms

range from physical solutions of the equation of radiative transfer to algorithms based completely upon statistical regression analysis. The absolute accuracies, as compared to in situ data, vary from approximately 1 deg. Kelvin for the single band direct solution algorithm to a few tenths of a Kelvin for the split-window algorithms (Pedersen 1982).

Weinreb & Hill (1980) describe an algorithm applying single band thermal infrared data. From the general equation of radiative transfer in an attenuating medium (cf. equation 1), the absolute surface temperature is derived after having corrected for the atmospheric influence. The atmospheric correction is calculated from an input of atmospheric temperature- and humidity profiles. This algorithm has been implemented for operational use at Tromsø Satellite Station (Pedersen 1982).

For testing the implemented SST algorithm, a NOAA data set from the summer 1981 covering the island Jan Mayen was applied (see Fig. 3) (Pedersen 1982). Radiosonde data from the meteorological station at the island were applied as input for atmospheric corrections of the satellite data. In situ SST measurements from the area around Jan Mayen made by ships were also available from the Norwegian Institute for Marine Research.

The resulting atmospheric corrected SST image is presented in Fig. 4. The scale at the top of the image gives the relationship between the grey levels and the surface temperatures. The scale number 1.25 means that the surface temperature is within the range 1–1.5 deg. centigrade. The island Jan Mayen is located almost in the centre of the image. Comparisons of the satellite and the in situ temperatures show an average absolute difference of 1 deg Kelvin. For all comparisons, the satellite measurements were systematically below the in situ measurements. The observed difference agrees well with the commonly accepted error achievable from a physical model, single thermal infrared band algorithm (Pedersen 1982).

The increased spatial resolution of the TM thermal infrared channel, as compared to the AVHRR, offers the possibility of applying the TM for studies of the surface temperatures in the coastal zone and within the fjords. The image presented in Fig. 5 is a Landsat-5/TM thermal infrared sub-scene covering the Tromsø area. Tromsø is located in the upper right corner of the

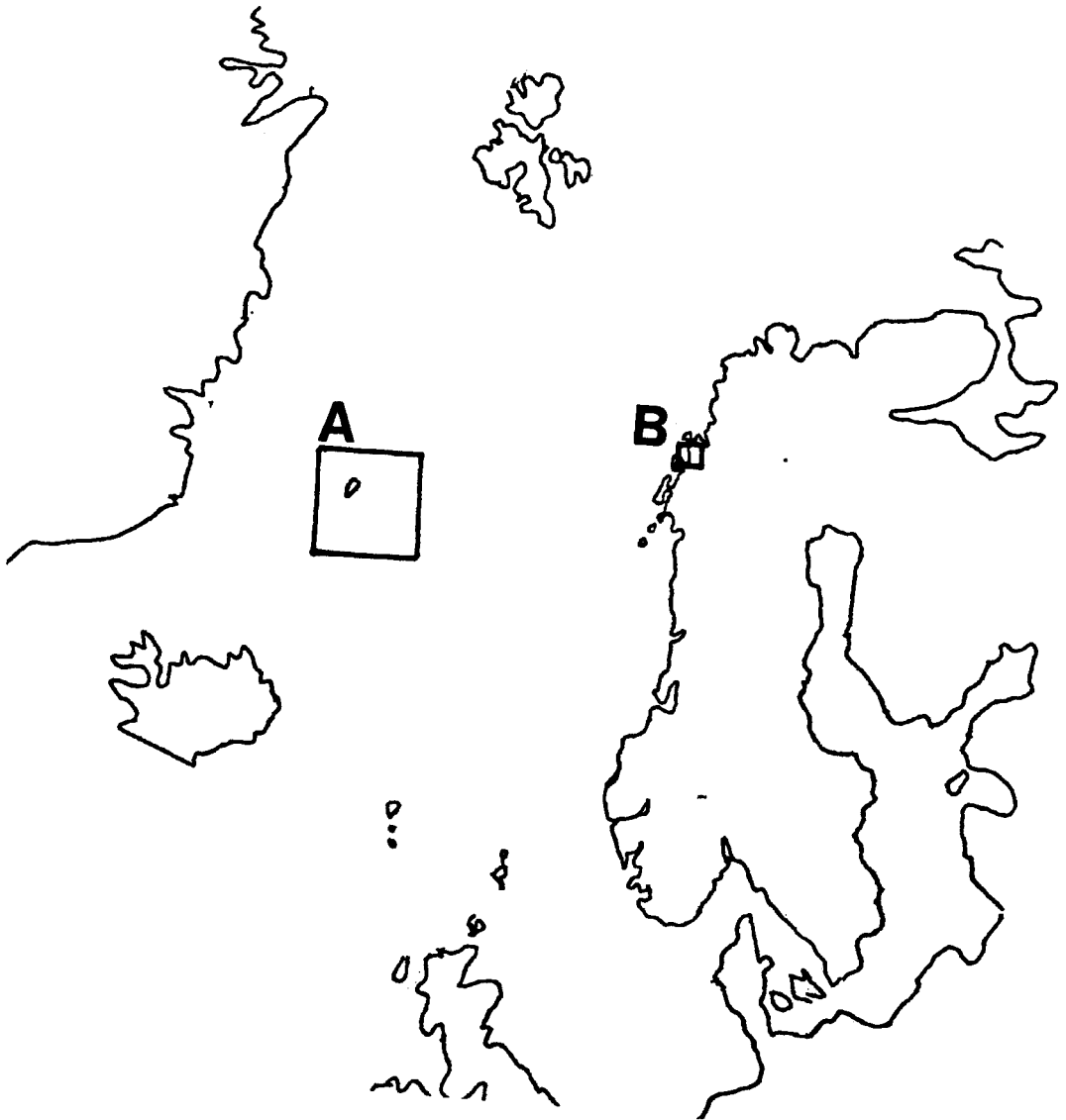


Fig. 3. Approximate geographical location of data sets presented in this paper. A = Jan Mayen, B = Tromsø.

image. The scale in the bottom left corner gives the correspondence between the grey levels and the surface temperatures. The colour-temperature scale was calibrated using surface temperatures measured at known image locations. By combining the thermal infrared band with a near-infrared band (0.76–0.90  $\mu\text{m}$ ), areas of land have been blanked out.

When the data set was acquired (3 June 1984), the sea current around the island Tromsø was

moving north (up in the image). Relatively warm surface water (c. 10 deg. centigrade) is transported upwards from Balsfjord (centre right in the image). Two bridges extend from the island of Tromsø, one to the east and one to the west. As the water flows under the bridges, the supports cause a turbulent mixing of the warm surface water with the colder sub-surface water which is clearly observed in the image.

In the centre of the image, there is an area



Fig. 4. SST image from Jan Mayen (centre of image). Image based on NOAA/AVHRR data read out at Tromsø Satellite Station 20 August 1981. The scale at the top of the image gives the relationship between the grey levels and the temperatures. A scale value of e.g. 1.25 means that the surface temperature is within 1. and 1.5 deg. centigrade.

where the surface water temperature is approximately 2–3 deg. below that of the surrounding areas. This is caused by strong turbulence in the narrow sound between the two large islands. Notice also that there is a small island located in

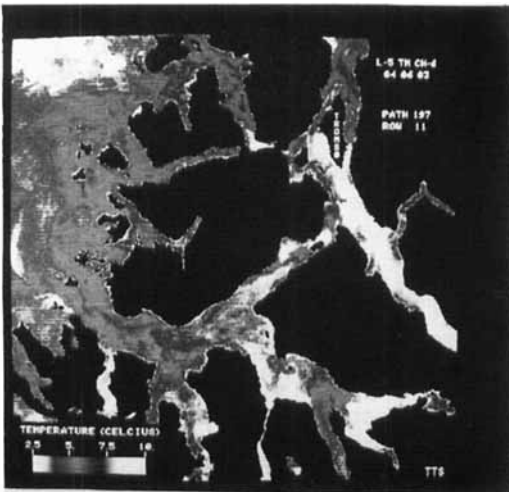


Fig. 5. Landsat-5/Thematic Mapper SST image covering the Tromsø area. Data read out at Kiruna read out station 3 June 1984. For discussion of the image, see the text.

the sound which strongly influences the water transport through the sound.

In the bottom right of the image, a fjord which is an outlet for cold water can be seen. The cold water results from the river Målselva transporting cold snow-melt water from the nearby mountains into the fjord.

### Conclusions

Ocean colour and surface temperature studies are best performed using optical remote sensing data. The major limitation regarding the optical data availability is the dependence upon the weather conditions. Darkness and/or cloud cover strongly limit the data acquisition. Experience from optical remote sensing in arctic regions show that, on average, there are only a few days during the year which are completely cloud free over large areas. Despite these limitations, a number of important and interesting optical remote sensing applications have been demonstrated.

The results obtained from NIMBUS/CZCS data for ocean colour studies indicate that this category of remote sensing data represents an important potential for the mapping of the productivity of remote, but important, ocean areas. The atmosphere represents the major problem in order to obtain acceptable geophysical data accuracy for operational applications. The atmosphere is a temporary and spatially varying medium, and the variations can not be given from a known law. In each case, the atmosphere needs to be described and the variations detected before reliable atmospheric corrections of the sub-surface data can be obtained.

For SST studies, the medium-resolution NOAA/AVHRR have been very useful in the research towards a better understanding of oceanic processes. Although the coastal current off the western coast of Norway has been known for long, NOAA/AVHRR surface temperature data offered the possibility to perform simultaneous, multitemporary large area current studies. Satellite data combined with model studies have increased the understanding of the coastal current generation mechanisms which is a combination of hydrographical and meteorological conditions. This research has resulted in an operational system for coastal current forecasting.

A number of algorithms are available for the SST generation. The single band, physical model

achieves an accuracy of approximately 1 deg. Kelvin, while the multiple band algorithms claim an accuracy of a few tenths of a Kelvin (Pedersen 1982). The results presented in this paper show that the satellite derived surface temperatures are consistently below the ship measured temperatures. This is a very important result, and the absolute accuracy may for example be enhanced by the addition of a bias term into the algorithm. The reason for not applying a bias term in this algorithm was primarily to understand and demonstrate the single band physical model for radiative transfer at thermal infrared wavelengths in a coupled sea-atmosphere-sensor system (Pedersen 1982).

The medium resolution of the AVHRR data limits the applications mainly to open ocean areas. The improved resolution of the Landsat/TM offers the possibility to perform SST studies in the coastal zone and within the fjords. These applications have become more and more important during recent years, because of the increased economical exploitation of the coastal areas.

## References

- Gordon, H. R. & Clark, D. K. 1980: Atmospheric effects in the remote sensing of phytoplankton pigments. *Bound. Layer Meteorology* 18, 299-313.
- Gordon, H. R., Clark, D. K., Brown, J. W., Brown, O. B., Evans, R. H. & Broenkow, W. W. 1983: Phytoplankton pigment concentrations in the Middle Atlantic Bight: comparison of ship determinations and CZCS estimates. *Applied Optics* 22(1), 20-36.
- Guzzi, R., Rizzi, R. & Zibordi, G. 1987: Atmospheric correction of data measured by a flying platform over the sea: elements of a model and its experimental validation. *Applied Optics* 26(15), 3043-3051.
- Liou, K. 1980: *An Introduction to Atmospheric Radiation*. Academic Press Inc., New York.
- Maul, G. A. 1981: Application of GOES Visible-Infrared Data to Quantifying Mesoscale Ocean Surface Temperatures. *J. Geophys. Res.* 86(C9), 8007-8021.
- NASA 1984a: A Prospectus for Thematic Mapper Research in the Earth Sciences. *NASA Technical Memorandum 86149*. NASA, GSFC, Greenbelt, Md.
- NASA 1984b: *Phytoplankton & Surface Patterns*. NASA, JPL 400-221 2/84.
- NASA 1984c: *Tuna Catch & Ocean Color*. NASA, JPL 400-22J 2/84.
- Pedersen, J.-P. 1982: *Atmospheric effects on infrared sea-surface temperature measurements from satellites*. Cand. real. thesis, Univ. of Tromsø (in Norwegian).
- Pedersen, J.-P. 1987: A model for estimation and removal of the atmospheric effects on Landsat/Thematic Mapper subsurface water radiances. *Internal report. IMR, Univ. of Tromsø*.
- Schwalb, A. 1979: The TIROS-N/NOAA Satellite Series. *NOAA Technical Memorandum NESS 95*.
- Swain, P. & Davis, S. 1978: *Remote sensing: The quantitative approach*. Addison-Wesley Publ. Company, Reading, Mass.
- Sturm, B. 1982: The atmospheric correction of remotely sensed data and the quantitative determination of suspended matter in marine water surface layers. *Paper presented at Remote Sensing Summer School at Dundee, Scotland*.
- Weinreb, M. P. & Hill, M. L. 1980: Calculation of Atmospheric Radiances and Brightness Temperatures in Infrared Window Channels of Satellite Radiometers. *NOAA Technical Report NESS 80*.

